ResearchGate

See discussions, stats, and author profiles for this publication at: https://www.researchgate.net/publication/231371099

Effect of Synthetic Parameters on Structural, Textural, and Catalytic Properties of Nanocrystalline Sulfated Zirconia Prepared by Sol–Gel Technique

ARTICLE *in* INDUSTRIAL & ENGINEERING CHEMISTRY RESEARCH · OCTOBER 2003

Impact Factor: 2.59 · DOI: 10.1021/ie030099t

CITATIONS
66

READS
49

3 AUTHORS, INCLUDING:

Beena Tyagi
Central Salt and Marine Chemicals Research …
47 PUBLICATIONS **926** CITATIONS
SEE PROFILE

Raksh Vir Jasra
Reliance Industries Limited
328 PUBLICATIONS **5,523** CITATIONS
SEE PROFILE

Available from: Beena Tyagi
Retrieved on: 01 February 2016

Effect of Synthetic Parameters on Structural, Textural, and Catalytic Properties of Nanocrystalline Sulfated Zirconia Prepared by Sol−Gel Technique

Manish. K. Mishra, Beena Tyagi,* and Raksh. V. Jasra*

Silicates and Catalysis Discipline, Central Salt and Marine Chemicals Research Chemicals Institute, G.B. Marg, Bhavnagar, 364 002, India

A series of sulfated zirconia samples were synthesized by a two-step sol−gel technique using zirconium propoxide as a precursor having two different concentrations, hydrolyzed with aqueous ammonia at pH 9−10 and sulfated with sulfuric acid. Effects of various synthetic parameters were studied on the structural, textural, and catalytic properties, which were determined using XRD, FT-IR, DRIFT, N_2 adsorption−desorption isotherms, and benzylation of toluene. The sol−gel technique resulted in the formation of nanocrystalline sulfated zirconia having a low crystallite size (<20 nm) predominantly in the tetragonal phase with a surface area and pore size ranging from 64 to 116 m^2/g and 47−67 Å, respectively. The amount of sulfur and the nature of the sulfur species bound with the zirconia surface were observed to play a significant role in determining the catalytic activity of a sample. Ultrasonication assisted sulfated zirconia samples prepared with a higher concentration of the metal precursor were found to be superior in higher sulfur loading and dispersion and thus had higher catalytic activity for the benzylation of toluene. Under the reaction conditions studied, benzylation of toluene was carried out by the sulfur species having an ionic configuration, which is attributed to a high sulfur content.

1. Introduction

Solid acid catalysts have many advantages over conventionally used acid catalysts such as H_2SO_4 and HF in the sense that these are recoverable, reusable, and required in catalytic amounts. As a result, solid acid catalysts are emerging as eco-friendly substitutes[1] to hazardous mineral acids and Friedal-Craft catalysts such as $AlCl_3$. Many of the single metal oxides are weakly acidic and have been modified for developing solid acid catalysts. For example, some sulfated-metal oxides exhibit acidity that can catalyze organic reactions such as isomerization, alkylation, and acylation. Among these, sulfated zirconia has been reported to show superacidity and is a potential catalyst for *n*-butane isomerization.[2,3] However, the catalytic activity of sulfated zirconia is strongly influenced by the method of its preparation that affects the structural and textural features of the catalyst, which are responsible for catalytic activity.[4−6]

Sulfated zirconia (SZ) has generally been prepared by a conventional precipitation method and occasionally by the sol−gel method. The samples prepared by the sol−gel technique have high sulfur content,[7] higher concentration of anionic vacancies,[8] give tetragonal zirconia phase[9] on heating amorphous $Zr(OH)_4$, and show interesting catalytic activity.[10] Both the precipitation and sol−gel techniques may result to form nanocrystalline zirconia.[8,9,11] However, the latter is advantageous due to the ease of controlling homogeneity and physical characteristics during the synthetic steps of the process to form genuinely nanocrystalline material.[12,13] A nanocrystalline material may have a strong effect on catalytic properties due to a large surface-to-volume ratio and the variation in geometrical and electronic structures.[14,15] Therefore, application of nanocrystalline sulfated zirconia as a catalyst or catalyst support is promising and worth exploring.

In general, the sol−gel process involves the formation of a sol by the hydrolysis and condensation of the precursor, especially metal alkoxide. The condensation of sol particles into a three-dimensional network produces a gel, and drying of gel results into the formation of a solid product. Various parameters involved during the synthesis of a gel affect its structural and textural features. A number of studies have been carried out to see the effect of parameters such as precursor concentration, drying, and calcination temperature.[16−19] However, the effects of physical perturbation on the structural and textural and thus the catalytic activity of sulfated zirconia have not yet been studied. The role of physical perturbation during the hydrolysis and condensation steps might influence the structural and textural properties of the sample. In the present paper, we report the effect of different parameters such as concentration of precursor, drying temperature, and calcination temperature on the structural (crystallinity, binding of sulfate ions, and average crystallite size) and textural properties (surface area and pore size distribution) of sulfated zirconia. Ultrasonication assisted synthesis of a series of sulfated zirconia by the two-step sol−gel technique with zirconium propoxide [$Zr(OC_3H_7)_4$] as a precursor was studied. For comparison, samples using conventional physical perturbation by a magnetic stirrer, during the hydrolysis and condensation process, were also prepared. The effect of all these parameters on the catalytic activity of the samples prepared was studied by carrying out the benzylation of toluene with benzyl chloride.

* To whom correspondence should be addressed. Phone: 91-278-2471793. Fax: 91-278-2567562; 91-278-2566970. E-mail: salt@csir.res.in; rvjasra@csir.res.in.

10.1021/ie030099t CCC: $25.00 © 2003 American Chemical Society
Published on Web 10/15/2003

Table 1. Synthetic Parameters of Sulfated Zirconia Samples Prepared[a]

sample code	precursor conc (wt %)	hydrolyzing agent	stirring mode and time	drying temp (K)	calcination temp (K)
SZ-1 (873)	70	$H_2O + NH_3$	MS, 2 h	298	873
SZ-2 (873)	70	$H_2O + NH_3$	MS, 2 h	353	873
SZ-3 (873)	70	$H_2O + NH_3$	MS, 8 h	383	873
SZ-3 (773)	70	$H_2O + NH_3$	MS, 8 h	383	773
SZ-4 (773)	10	NH_3	MS, 8 h	383	773
SZ-7 (873)	10	NH_3	US, 1/2 h	383	873
SZ-6 (873)	10	NH_3	US, 1 h	383	873
SZ-11 (873)	10	NH_3	US, 2 h	383	873
SZ-14 (873)	70	NH_3	US, 2 h	383	873

[a] SZ = sulfated zirconia, MS = magnetic stirring, US = ultrasonication.

2. Experimental Section

2.1. Materials. Zirconium propoxide, $[Zr(OC_3H_7)_4]$, in 1-propanol was procured from Sigma-Aldrich; concentrated H_2SO_4, 1-propanol, aqueous ammonia (25%), toluene, and benzyl chloride were from s.d. Fine Chemicals, India, and were used as such.

2.2. Catalyst Preparation. Sulfated zirconia samples were prepared by a two-step sol−gel technique. Typically, hydrolysis of $[Zr(OC_3H_7)_4]$ at pH 9−10 was performed with water and aqueous ammonia at room temperature (298 K) followed by drying of the resulting $Zr(OH)_4$ gel at room temperature and then at 353 or 383 K in the first step. This was followed by sulfation in the second step by stirring the powdered (170-mesh) sample with concentrated H_2SO_4 (0.5 M, 15 mL/g) for 30 min. Thus prepared samples were dried at room temperature and then at 383 K for 12 h after filtration.

$[Zr(OC_3H_7)_4]$ solutions used were of 70 and 10 wt % in propanol. For hydrolysis, a 1:4 ratio of $[Zr(OC_3H_7)_4]$ to water was used. Physical perturbation during the hydrolysis and condensation was carried out by ultrasonication or magnetic stirring. Ultrasonication was performed by an ultrasonic cleaner (Cole Parmer model 8891) having 47 kHz sound wave frequency for 30 to 120 min. Magnetic stirring was done by a magnetic stirrer (Mirak Thermolyne) at 600−1100 rpm. Samples were calcined at different temperatures ranging from 673 to 873 K for 3 h in a muffle furnace in air atmosphere. Synthesis parameters of all the samples prepared are summarized in Table 1. In the sample nomenclature used, SZ stands for sulfated zirconia, Z is for pure zirconia, numbers 1−14 are for laboratory experimental serial number, and the number given in parentheses is for the calcination temperature in Kelvin degree.

2.3. Characterization. 2.3.1 X-ray Powder Diffraction (XRD) Studies. The crystalline phase formed and the crystallinity of sulfated and nonsulfated zirconia were measured by X-ray powder diffractometer (Philips X'pert) using CuKα radiation (λ = 1.5405 Å). The samples were scanned in 2θ range of 0 to 70 deg at a scaning rate of 0.4 deg/s. Crystallite size of tetragonal phase was determined from the characteristic peak (2θ = 30 for the (111) reflection) using the Scherrer formula,[20] with a shape factor (K) of 0.9

$$\text{crystallite size} = K\lambda/W\cos\theta \qquad (1)$$

where

$$W = W_b - W_s \qquad (2)$$

and W_b = broadened profile width of experimental sample and W_s= standard profile width of reference silica sample.

The quantification of the tetragonal and monoclinic phase present in the zirconia was done[21] by comparing the areas of the characteristic peaks of the tetragonal phase (2θ = 30 for the (111) reflection) and the monoclinic phase (2θ = 28 and 31 for $(11\bar{1})$ and (111) reflection, respectively). The percent composition of each phase was calculated from the areas, hw, where h and w are the height and the half width of the X-ray diffraction pattern at the characteristic peaks.

$$\%\ \text{tetragonal} = [(hw)\ \text{tetragonal}/\Sigma(hw)\ \text{tetragonal and monoclinic}] \times 100$$

$$\%\ \text{monoclinic} = [(hw)\ \text{monoclinic}/\Sigma(hw)\ \text{tetragonal and monoclinic}] \times 100$$

2.3.2. (a) FT-IR Spectroscopic Studies. The nature of bonding of sulfate ions with the zirconia surface before and after calcination at different temperatures was studied by FT-IR spectrophotometry (Perkin-Elmer GX spectrophotometer). The spectra were recorded in the range 400−4000 cm^{-1} with a resolution of 4 cm^{-1} as KBr pellets.

(b) Diffuse Reflectance FT-IR (DRIFT) Studies. The effect of in-situ heating on the nature of the sulfate species formed on the zirconia surface was determined by using an FTIR spectrophotometer equipped with The Selector DRIFT accessory (Graseby Specac, P/N 199900 series) incorporating an environmental chamber (EC) assembly (Graseby Specac, P/N 19930 series). The spectra were recorded for sample diluted with KBr (similarly as in KBr pellets) in the range of 400−4000 cm^{-1}. The reference spectrum was recorded with KBr. The spectra were recorded at room temperature and after in situ heating at different temperatures (423−723 K) using an automatic temperature controller (Graseby Specac, P/N 19930 series) connected with the EC at a heating rate of 298 K/min and at 1 atm pressure. Samples were kept at each temperature for 30 min, thus allowing sufficient time for water vapor desorption. Typically, 30 scans were co-added at a resolution of 4 cm^{-1}. All the spectra were recorded under dry N_2 flow (30 $cm^3\ min^{-1}$).

2.3.3. Surface Area and Pore Size Distribution. Specific surface area, pore volume, and pore size distributions of calcined sulfated and nonsulfated zirconia samples were determined from N_2 adsorption−desorption isotherms at 77 K (ASAP 2010, Micromeritics, USA). Surface area and pore size distribution were determined using the BET equation and BJH method,[22] respectively. The samples were degassed under vacuum at 393 K for 4 h, prior to measurement, to evacuate the physiosorbed moisture.

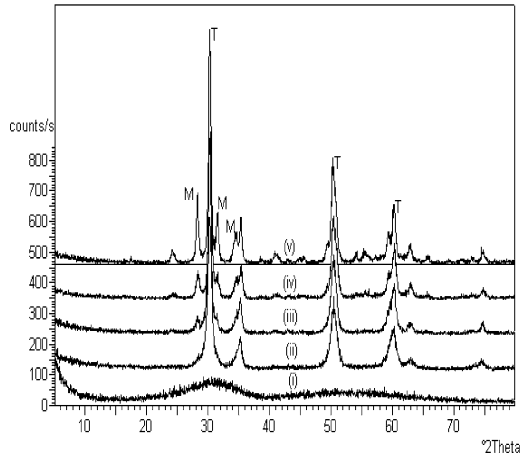

Figure 1. X-ray diffraction of ZrO_2 (Z-3) sample (i) before calcination (383 K) and after calcination at (ii) 673 K, (iii) 723 K, (iv) 773 K, (v) 873 K.

2.3.4. Thermal Analysis. Thermogravimetric analysis (TGA) and differential thermal analysis (DTA) were performed using simultaneous DSC/TGA (TA Instruments, model SDT 2960). Samples were scanned in the temperature range of 298−1273 K with a heating rate of 283 K/min under air flow (100 cm^3 min^{-1}).

2.3.5. Sulfur Analysis. Percentage of sulfur retained in sulfated zirconia samples after calcination at 773 or 873 K was analyzed by a CHNS/O elemental analyzer (Perkin-Elmer, 2400).

2.4. Catalytic Activity. Benzylation of Toluene. The catalytic activity of the sulfated zirconia samples prepared was determined by benzylation of toluene with benzyl chloride in liquid phase. In a double neck round-bottom flask, toluene and benzyl chloride were taken in a 1:1 molar ratio, and the catalyst (activated at 723 K for 2 h) was added to the mixture. Average particle size of the catalysts as determined by the light scattering method using Master Sizer 2000 (Malvern Instruments, Ltd, U.K.) was in the range of 20−55 microns. Toluene and catalyst, by weight, were taken in a 10:1 ratio. The reaction was carried out at 383 K with N_2 atmosphere. The reaction solution was stirred well at 600 rpm. Under these conditions, the solution was well agitated, and there will not be any mass transfer resistance due to liquid film formed around the external surface of the catalyst. The reaction mixture was analyzed at various intervals by gas chromatography (HP6890) having a HP50 (50-m long) capillary column with a programmed oven temperature from 323 to 473 K and a 0.5 cm^3 min^{-1} flow rate of N_2 as carrier gas. To arrive at the optimum time for the maximum conversion, the kinetics was measured for one of the samples, SZ-14. Conversion data show that the reaction is completed within 4 h. Therefore, the catalytic activity for the other samples was studied after 4 h and conversion data are tabulated in Table 4. GC peak areas were calibrated using standard mixtures for calculating wt % from GC peak area percentages.

3. Results and Discussion

3.1. Structural Properties. 3.1.1 Crystalline Phase. X-ray diffraction patterns of pure zirconia (Z-3) samples before calcination (dried at 383 K) and after calcination at temperatures of 673, 723, 773, and 873 K are given in Figure 1. The sample before calcination was observed to be predominantly amorphous in nature. The sample, calcined at 673 K, had only a tetragonal phase, whereas the samples calcined at >673 K contained both tetragonal and monoclinic phases. Percentage of crystalline phases observed at different calcination temperatures given in Table 2 shows that the monoclinic phase progressively increases from 4 to 29% with an increase in the calcination temperature from 723 to 873 K. It is evident from these data that the calcination temperature of the amorphous zirconia has a significant influence on the zirconia phase formed. The zirconia sample obtained on heating at 383 K is a $Zr(OH)_4$ gel that is of amorphous nature which develops crystallinity on thermal treatment at higher temperatures. Transformation of amorphous $Zr(OH)_4$ gel occurs first to a metastable tetragonal and then to a monoclinic crystalline phase of ZrO_2. In pure amorphous zirconia, the initial crystallization to a tetragonal phase is observed to occur at about 673 K. The main peak of the amorphous phase had the same position as the main peak of the tetragonal phase corresponding to (111) reflection showing the similar local order in both phases. Calcination at temperature >673 K results in the transformation of a tetragonal to monoclinic phase due to the loss of −OH ions that are known to stabilize the tetragonal structure[9] and thus results in a mixture of both tetragonal and monoclinic phases of zirconia.

Table 2. Crystalline Phase and Crystallite Size of Sulfated and Pure Zirconia Samples[a]

sample code	phase (%) T	phase (%) M	crystallite size (nm)	S (wt %) after calcination
SZ-1(873)	11	89		
SZ-2 (873)	100		10.0	1.18
SZ-3 (873)	78	22	16.0	1.35
SZ-3 (773)	94	6	17.0	0.87
SZ-4 (773)	99	1	15.0	0.93
SZ-7 (873)	96	4	13.0	0.78
SZ-6 (873)	96	4	12.0	0.99
SZ-11(873)	100		13.0	1.77
SZ-14(873)	100		15.0	1.91
Z-3 (673)	100		13.0	
Z-3 (723)	96	4	18.0	
Z-3 (773)	83	17	20.0	
Z-3 (873)	71	29	23.0	

[a] SZ = sulfated zirconia, Z-3 = pure zirconia.

Figure 2 shows the XRD pattern of sulfated zirconia samples calcined at 723, 773, and 873 K. The samples, calcined at 773 K, predominantly contained the tetragonal phase, above which a gradual increase of the monoclinic phase starts, whereas below 773 K the samples remain mainly amorphous. Table 2 includes the percentage of crystalline phases observed for different samples at different calcination temperatures. In sulfated zirconia, crystallization of an amorphous sample to a crystalline phase occurs at temperature (723 K) higher than that of pure sample (673 K). This is explained in terms of the presence of SO_4^{2-} ions, which necessitates into higher thermal energy requirement for the removal of OH^- ions.[8] Dehydroxylation of the amorphous phase at 773 K generated mainly tetragonal zirconia. Calcination at higher temperatures (between 773 to 873 K) results in the formation of the monoclinic phase as observed for pure zirconium oxide; however, the temperature, at which the transformation of tetragonal (t) to monoclinic (m) phase occurs is higher

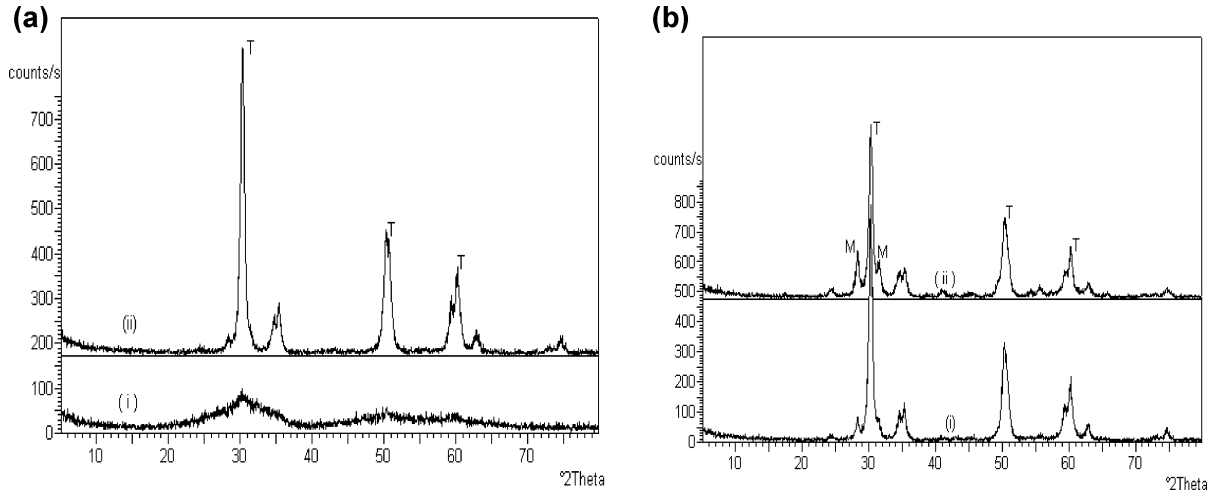

Figure 2. (a) X-ray diffraction of SZ sample (i) SZ-4 (723), (ii) SZ-4 (773). (b) X-ray diffraction of SZ sample (i) SZ-3 (773), (ii) SZ-3 (873).

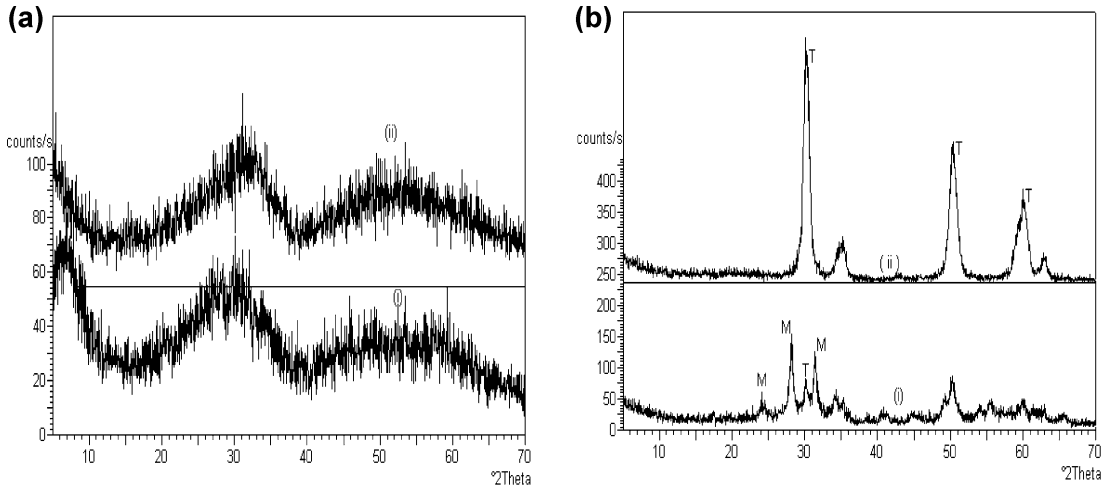

Figure 3. (a) X-ray diffraction of amorphous SZ sample (i) SZ-1 dried (298 K), (ii) SZ-2 dried (353 K). (b) X-ray diffraction of crystalline SZ sample (i) SZ-1 (873), (ii) SZ-2 (873) after calcination (873 K).

in sulfated zirconia as shown below:

$$Zr(OH)_4 \xrightarrow{673\ K} ZrO_2\ (t) + 2H_2O$$

$$ZrO_2\ (t) \xrightarrow{723-873\ K} ZrO_2\ (t) + ZrO_2\ (m)$$

$$SO_4^{2-}\text{-}Zr(OH)_4 \xrightarrow{773-873\ K} SO_4^{2-}\text{-}ZrO_2\ (t)$$

$$SO_4^{2-}\text{-}ZrO_2\ (t) \xrightarrow{>\ 873\ K} SO_4^{2-}\text{-}ZrO_2\ (t) + SO_4^{2-}\text{-}ZrO_2\ (m)$$

It has been reported that in the sol−gel technique the tetragonal phase is stabilized in a manner different from that in the conventional method. In the latter case, it is stabilized[23] by sulfate anions or large cations such as Ce^{3+}, Y^{3+}, Ca^{2+}, or Mg^{2+}, and in the sol−gel technique, the hydroxide ions stabilize[9] the tetragonal phase and the loss of these −OH ions during dehydroxylation at higher temperature transforms the tetragonal phase to the monoclinic phase. However, our observations of formation of the tetragonal phase at higher temperature (773 K) in sulfated samples as compared to pure zirconia samples (673 K) show that even in sol−gel zirconia, the sulfate ions contribute toward the stabilization of the tetragonal phase.

The phase obtained is reported to depend on the precursor used;[24] for example, monoclinic zirconia is obtained when $Zr(NO)_3$ is the precursor. In the present study, all the samples prepared using metal alkoxide as a precursor, amorphous gel formed initially transformed to the tetragonal phase. It is only at higher temperature at which the tetragonal phase transforms to the monoclinic phase.

It is seen from Table 2 that the sulfated zirconia samples, SZ-6, SZ-7, SZ-11, and SZ-14, prepared using ultrasonication result predominantly tetragonal phase even at a calcination temperature of 873 K. On the other hand, for the samples prepared using magnetic stirring, SZ-3 gives a substantial amount (22%) of monoclinic phase when calcined at 873 K. This shows higher thermal stability of the tetragonal phase in samples prepared using ultrasonication as compared to conventional stirring. This probably is due to higher loading and dispersion of sulfate ions on zirconia surface during ultrasonication, which is also confirmed by a higher percentage of sulfur (Table 2) retained by these samples as discussed in later sections.

It is also seen from Table 2 and Figure 3 that the samples initially dried at 353 or 383 K have a tetragonal phase (94−100%), whereas the sample dried only at room temperature, SZ-1, showed predominantly a monoclinic phase (89%) after calcination at 873 K. This is

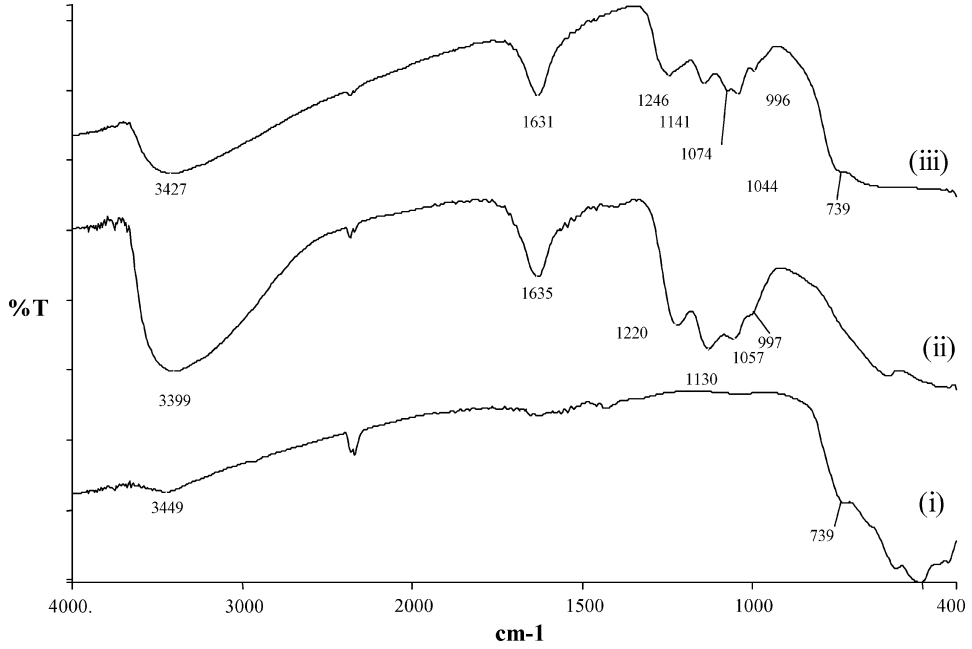

Figure 4. FT-IR spectra of zirconia sample (i) pure zirconia, (ii) SZ sample after drying at 383 K, (iii) SZ sample after calcination at 873 K.

explained in terms of the presence of propanol formed during the hydrolysis of the alkoxide, which does not get removed from the gel when the sample is only air-dried at ambient temperature. As the gel pores are filled with propanol, sulfate loading inside zirconia pores is adversely affected during the sulfation process. The reduced amount of sulfate ions in the gel results in the formation of the monoclinic phase as sulfate ions have been observed to stabilize the tetragonal phase.

3.1.2. Crystallite Size. Crystallite size determined from X-ray diffraction data showed (Table 2) that all zirconia samples, sulfated as well as nonsulfated, prepared by the sol−gel technique are of nanocrystalline size (10−23 nm). Furthermore, the crystallite size of pure tetragonal zirconia samples (Z-3's) increases progressively from 13 to 23 nm with an increase in calcination temperature (673−873 K), indicating the sintering of zirconia crystallites with temperature leading to larger crystallites. The crystallite size of sulfated tetragonal zirconia was observed to be smaller in comparison to pure zirconia. The dilute concentration of the precursor also results in the formation of crystallites of slightly lower size, either stirred by conventional (15 nm with 10% and 16−17 nm with 70%) or ultrasonication (13 nm with 10% and 15 nm with 70%) methods. In the present study, the samples (SZ-6, SZ-7, SZ-11, SZ-14) prepared by ultrasonication, in general, were found to be of slightly smaller crystallite size (12−15 nm) than those synthesized by the conventional method (15−17 nm) of physical perturbation. The sample SZ-2 was found to be the only exception having a low crystallite size (10 nm) with higher concentration and conventional stirring.

3.1.3. (a) FT-IR Studies. The FT-IR spectra of pure and sulfated zirconia samples dried at 383 K followed by calcination at 873 K are given in Figure 4. The sulfated zirconia samples dried at ambient temperature and 383 K showed the IR bands of the SO_4^{2-} group in the region of 1200−900 cm^{-1}, with peaks at 1220−1214, 1130−1128, 1060−1054, and 996 cm^{-1}, characteristic of inorganic chelating bidentate sulfate, which are assigned[25] to asymmetric and symmetric stretching

Scheme 1

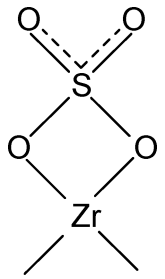

frequencies of S⁻⁻O and S−O bonds as shown in Scheme 1. This ionic structure shows the presence of Bronsted acid sites available in the sample. On calcination, the first two peaks shift toward higher wavenumber, namely, 1246−1220 and 1142−1138 cm^{-1}; the third peak either shifts to lower wavenumber at 1049−1044 cm^{-1} or splits into two peaks at 1074 and 1044 cm^{-1}. The fourth peak at 996 cm^{-1} remains at the same position. The shifting of IR bands on calcination indicates the formation of strong SO_4^{2-} bonding with the zirconia surface after the development of crystallinity within the sample.

A broad peak observed at around 3400 cm^{-1} is attributed to the ν_{O-H} stretching mode of water associated with zirconia, the broadness of which is due to a hydrogen bonding effect.[26] An intense peak at 1631−1635 cm^{-1} is attributed to δ_{O-H} bending mode of water associated[26] with the sulfate group.

Figure 5 shows the IR spectra of a sulfated zirconia sample calcined at 873 K, which was initially dried at ambient temperature or 353 K. After sulfation, the samples dried at room temperature or 353 or 383 K showed similar spectra as such. However, after calcination at 873 K, the sample dried at 353 K (Figure 5) or 383 K (Figure 4) showed the presence of bidentate chelating sulfate ions, whereas the sample dried at only ambient temperature showed a broad peak at 1130 cm^{-1}. It clearly indicates that the evaporation of solvent during drying of the gel plays an important role affecting the structure of the sulfate ion. The presence

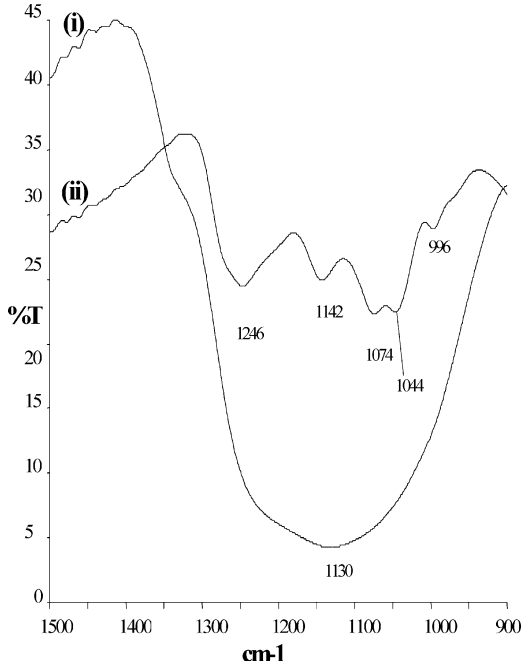

Figure 5. FT-IR spectra of SZ sample (i) SZ-1 (873), (ii) SZ-2 (873).

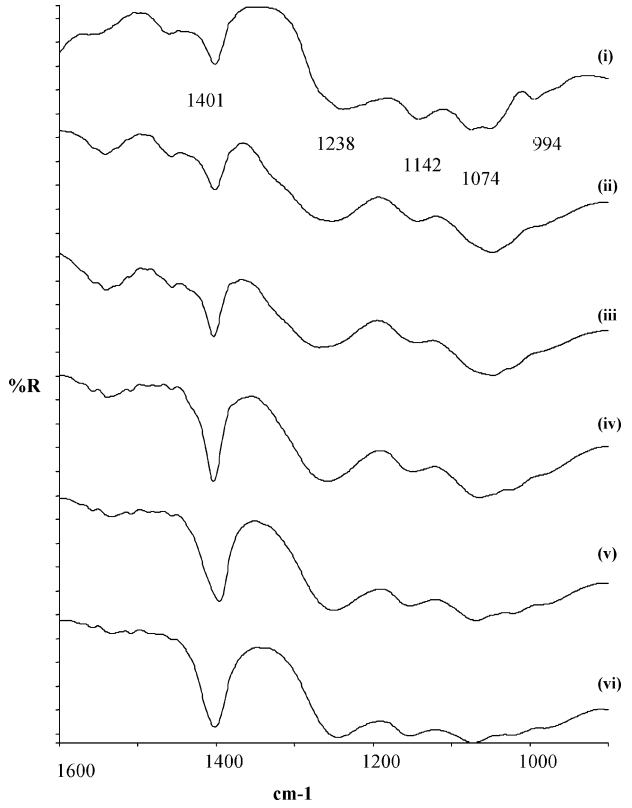

Figure 6. DRIFT spectra of calcined SZ sample recorded after in situ heating at different temperatures (i) RT, (ii) 423 K, (iii) 523 K, (iv) 573 K, (v) 673 K, (vi) 723 K.

of solvent (propanol) before sulfation may affect the bonding of sulfate ions with the zirconium atom.

3.1.3. (b) Diffuse Reflectance FT-IR Studies. Figure 6 shows the DRIFT spectra of calcined sulfated zirconia samples recorded after in situ heating at different temperatures. All prepared sulfated zirconia samples showed a weak to medium band at around 1401 cm^{-1} at ambient temperature, which is assigned[25,27] to asymmetric stretching of covalent $\nu_{S=O}$ band (Scheme 2). This structure corresponds to the Lewis acid sites available in the samples. The in situ heating of the samples at 423 K showed the increase in the intensity of $\nu_{S=O}$ peak at 1401 cm^{-1}, which further increases at higher temperatures. The broad peak of ν_{O-H} at 3400 cm^{-1} and δ_{O-H} at 1630 cm^{-1} has decreased substantially after heating at 423 K. This spectral change shows that the removal of molecular water resulted in the structural transformation from Bronsted acid sites (Scheme 1) to Lewis acid sites (Scheme 2). Similar observation was reported[25] for $SO_4^{2-}-Fe_2O_3$, wherein structure, having Lewis acid sites, was found essential for acid-catalyzed reactions. The increasing peak area of this band with increasing temperatures (Figure 7) shows the sensitivity of the $\nu_{S=O}$ peak towards the molecular water adsorbed on the surface of sulfated zirconia samples.[25,27]

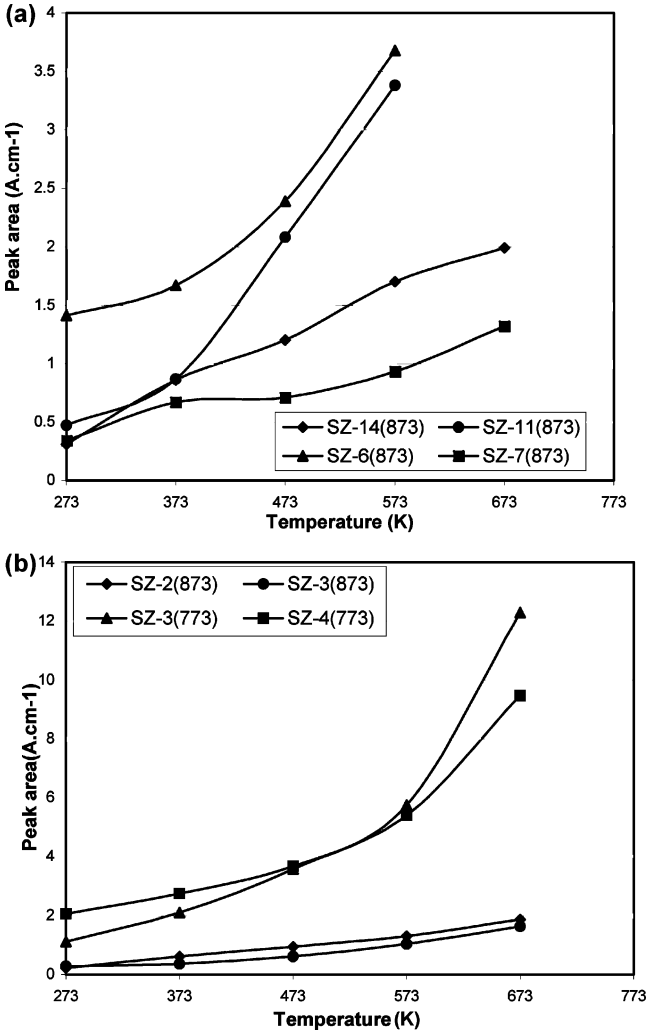

Figure 7. (a) Peak area of $\nu_{S=O}$ band of US assisted SZ samples at different temperatures. (b) Peak area of $\nu_{S=O}$ band of conventionally stirred SZ samples at different temperatures.

Scheme 2

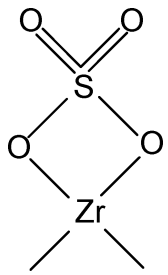

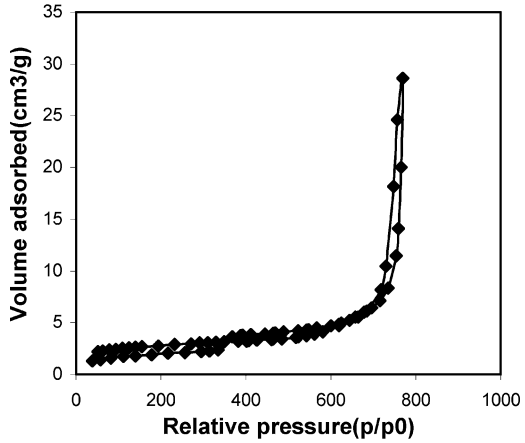

Figure 8. N_2 adsorption isotherm at 77 K for pure zirconia calcined at 873 K.

Table 3. Textural Properties of Sulfated and Pure Zirconia[a]

	surface area (m^2/g)		pore volume (cm^3/g)	pore size (Å)	
sample code	BET	BJH adsorption	BJH adsorption	BET (average pore size)	BJH adsorption
SZ-2 (873)	116	120	0.131	47	44
SZ-3 (873)	71	69	0.106	59	61
SZ-3 (773)	85	89	0.130	64	59
SZ-4 (773)	86	98	0.126	11	51
SZ-7 (873)	110	122	0.175	63	58
SZ-6 (873)	107	98	0.155	61	63
SZ-11 (873)	64	73	0.081	53	45
SZ-14 (873)	85	75	0.136	67	73
ASZ-2 (723)	41	34	0.084	83	98
Z-2 (873)	9.5	6.5	0.043	187	264

[a] SZ = sulfated zirconia, ASZ-2 = amorphous sulfated zirconia, Z-2 = pure zirconia.

Activation at 723 K results in more $\nu_{S=O}$ character, i.e., Lewis acidity. The peak area of $\nu_{S=O}$ covalent band has been correlated with the total sulfur present on the catalyst and the catalytic activity of the individual catalyst for the benzylation of toluene and is discussed in later sections.

3.2. Textural Properties. N_2 adsorption isotherm at 77 K measured for pure zirconia calcined at 873 K (Figure 8) was observed to be of type III, indicating the nonporous nature of the material which is also seen from its low surface area (6−9 m^2/g) and pore volume (0.043 cm^3/g) (Table 3). N_2 adsorption isotherms for amorphous sulfated zirconia samples calcined at 723 K (Figure 9a) indicate the presence of mesopores. Low surface area (25−41 m^2/g) and higher pore volume (0.084 cm^3/g) also indicates the presence of large mesopores. N_2 adsorption isotherms for crystalline sulfated zirconia samples, calcined at 773−873 K were found to be of type IV, typically observed for mesopores solids (Figure 9b). However, there is a large increase in adsorption at higher relative pressure (p/po) showing the presence of larger size mesopores in these solids. The inflection point observed in the N_2 adsorption isotherm at around p/po = 0.4 shows the capillary condensation within the mesopores after the formation of monolayer. This inflection in all the samples was not sharp, reflecting that the pores are not of uniform size and have broad distribution. Hysteresis in all samples prepared was observed to be of H2 or H3 type. H2 hysteresis is generally associated with complex pore structure. H3 hysteresis does not exhibit any limiting adsorption at high relative pressure and indicates that adsorbent does not possess any well-defined pore structure.

The surface area calculated from the adsorption isotherm using the BET equation as well as the BJH model is given in Table 3. Crystalline sulfated zirconia samples show higher surface area (71−116 m^2/g) than amorphous sulfated zirconia (25−41 m^2/g) and pure zirconia (6−9 m^2/g). The surface area increases up to a certain calcination temperature after which it decreases with further increase in calcination temperature. Decrease in surface area with increased calcination temperature might be due to sintering of pores at increased temperature.

The pore size distribution in all the samples prepared was observed to be broad ranging from 20 to 100 Å (Figure 10).

N_2 adsorption data distinctly show that only crystalline sulfated zirconia show reasonably high surface area as well as defined mesoporosity. It is also observed from the data (Table 3) that the concentration of the precursor and mode of stirring do not have a significant effect on the surface area; however, among the samples prepared by ultrasonication it was found to be higher

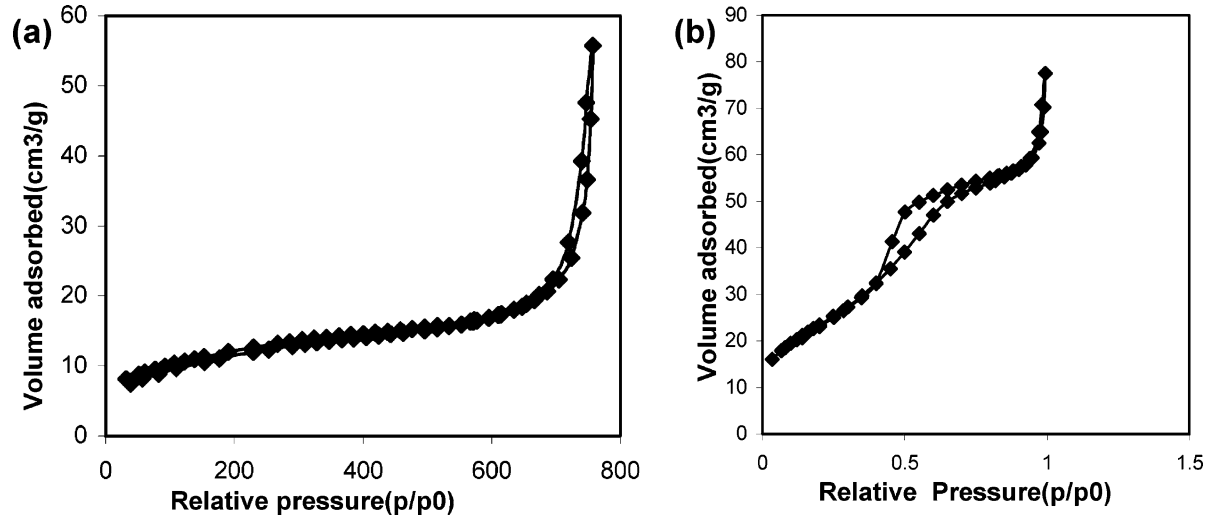

Figure 9. (a) N_2 adsorption isotherms for amorphous SZ samples calcined at 723 K. (b) N_2 adsorption−desorption isotherms for crystalline SZ samples calcined at 773−873 K.

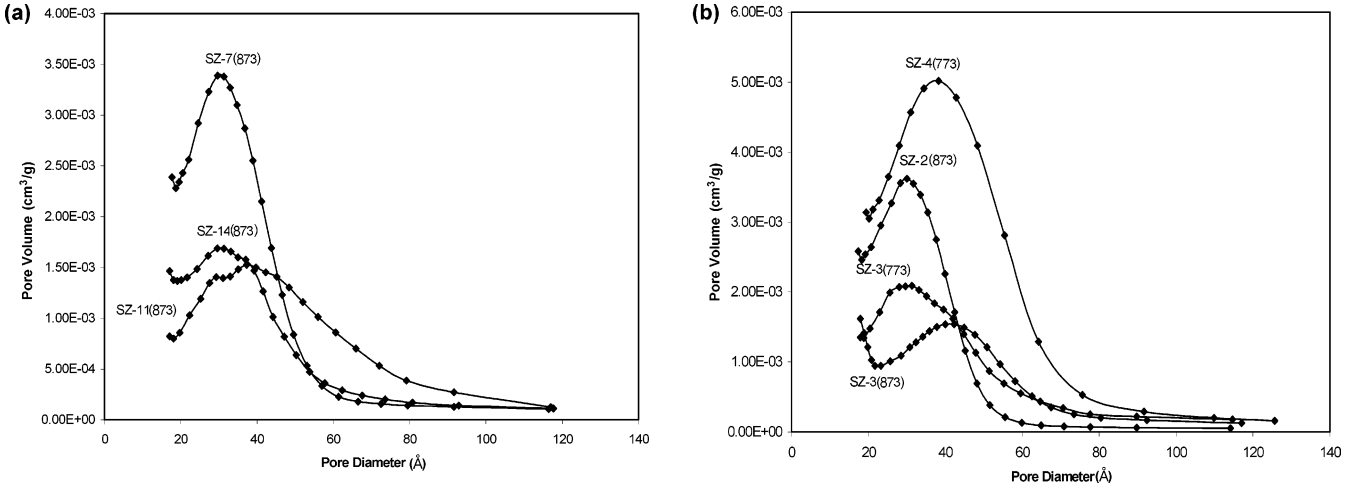

Figure 10. (a) The pore size distribution in US assisted SZ samples as determined from N_2 adsorption data using the BJH model. (b) The pore size distribution in conventionally stirred SZ samples as determined from N_2 adsorption data using the BJH model.

in samples prepared in 30 min (110 m^2/g) than those prepared in 2 h (64 m^2/g).

3.3. Thermal Analysis. In pure zirconia samples, the observed weight loss during calcination (773 K) of dried $Zr(OH)_4$ was 24 wt %. $Zr(OH)_4$, formed as per synthetic stoichiometry, loses 22.6 wt % water as per the following reaction:

$$Zr(OH)_4 \rightarrow ZrO_2 + 2H_2O$$

At higher calcination temperature (873 K), it increases to 33%, which may be due to dehydroxylation during the transformation of tetragonal to monoclinic phase of zirconia.

All sulfated zirconia samples prepared by changing various parameters and calcined at 773 and 873 K show 28 to 32 wt % weight loss. It shows that in sulfated zirconia samples the weight loss up to these temperatures is due to water loss during calcination and formation of oxide from hydroxide and not due to sulfate loss.

The above results were confirmed by thermal analysis (TGA and DTA) of the samples prepared showing sharp weight losses at 498 and 898 K. An endothermic peak at 313 K and exothermic peaks at 613 K and at higher temperatures 1173 K were observed. Thermal data distinctly show the initial water loss at lower temperature followed by a tetragonal to monoclinic transformation at higher temperature (starting at around 698 K) and sulfur loss at temperatures higher than 873 K.

3.4 Sulfur Analysis. Table 2 includes the percentage of sulfur in sulfated zirconia samples retained after calcination at 773 and 873 K. The data show the effect of concentration of the precursor, mode and duration of stirring on the sulfur loading, and retention after calcination. As seen from the sulfur data for samples SZ-3 (873) and SZ-14(873), ultrasonication resulted in higher sulfur retention in comparison to conventional stirring. Furthermore, the duration of ultrasonication was also found to affect the sulfur loading. As observed for samples SZ-7, SZ-6, and SZ-11, within the time period studied and keeping other conditions same, it increased from 0.78 to 1.77 wt % with the ultrasonication time increasing from 30 to 120 min. This may be due to higher dispersion of sulfur during ultrasonication, as ultrasonication results in more effective dispersion

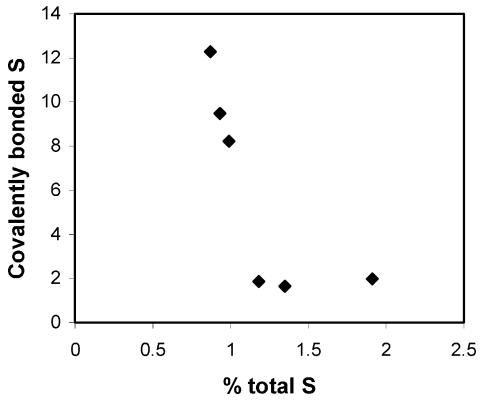

Figure 11. Variation of covalently bonded sulfur with total sulfur content.

of active sulfur over the supports.[28] However, nature of the sulfur species as observed from FT-IR studies was found to be same in all the samples.

The correlations of total sulfur with covalently bonded sulfur representing Lewis acid sites (peak area of $\nu_{S=O}$ band) shows an important observation that samples with <1.0% sulfur retention show higher Lewis acidity, whereas samples with >1.0% (1−2%) sulfur show lower Lewis acidity (Figure 11). It confirms the reported observation that lower sulfur loading results in Lewis sites and higher sulfur loading results into Bronsted sites.[29]

3.5. Catalytic Activity. Table 4 shows the conversion and selectivity data for the benzylation of toluene with different sulfated zirconia samples under similar reaction conditions. Ultrasonicated samples, SZ-14, showed higher catalytic activity among all the samples studied. Samples prepared from a higher concentration (70%) of the precursor showed higher activity irrespective of method of stirring in comparison to samples prepared with a lower (10%) concentration of the precursor.

3.5.1. Correlations of Catalytic Activity with Total Sulfur, Covalently Bonded Sulfur, and Surface Area. Figure 12a shows that % conversion for benzylation of toluene is linearly dependent on the sulfur content of the sample. However, the surface areas (Table 3) for these samples do not show any trend. Ultrasonicated sample having the lower surface area display higher catalytic activity showing that surface area alone does not influence the catalytic activity.

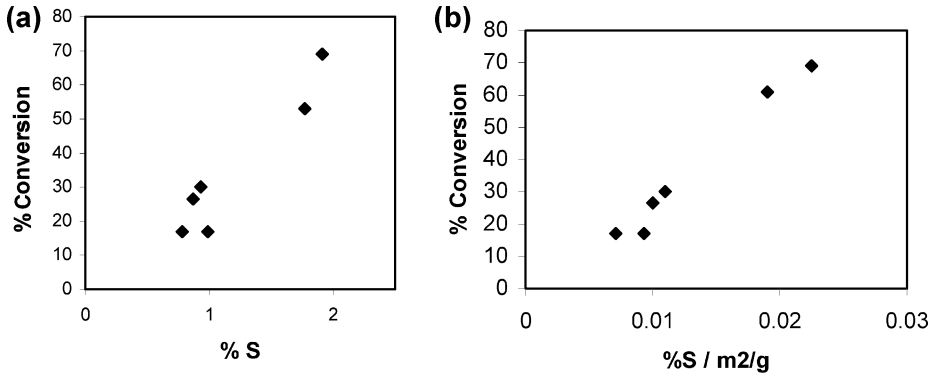

Figure 12. (a) Correlation of catalytic activity for benzylation of toluene with sulfur content of zirconia. (b) Correlation of catalytic activity with sulfur/surface area.

Table 4. Benzylation of Toluene with Sulfated Zirconia Samples

catalyst	time (h)	conversion (%)	selectivity (%) for *p*-benzyl toluene
SZ-3 (873)	4	61	100
SZ-3 (773)	4	27	100
SZ-4 (773)	4	30	100
SZ-7 (873)	4	17	100
SZ-6 (873)	4	17	100
SZ-11 (873)	4	53	100
SZ-14 (873)	4	69	100
	kinetics data for SZ-14		
	0.5	46	100
	1	48	100
	2	51	100
	3	56	100
	4	68	100
	5	66	100
	6	67	100

[a] Benzylating agent = benzyl chloride, toluene:benzyl chloride = 1:1 molar ratio, catalyst: toluene = 10:1 ratio by weight, reaction temperature = 383 K.

Thus, the amount of sulfur and the nature of the sulfur bound with the zirconia surface play rather a significant role in determining the catalytic activity of a sample. Therefore, to observe the effect of sulfur alone, total % sulfur per unit surface area was determined and plotted against % conversion for benzylation of toluene (Figure 12b) observed for various samples. This plot clearly shows the linear dependence of the catalytic activity with the sulfur per unit area of the sample.

Further to ascertain the role of the nature of the sulfur species on the catalytic activity, % benzylation conversion against Lewis acid sites or covalently bonded sulfur (peak area of $\nu_{S=O}$ band) was plotted (Figure 13). These data show that an increase in covalently bonded sulfur results in a decrease in benzylation activity of the samples for toluene. However, we have observed above (Figure 12) that the catalytic activity of the sulfated zirconia samples increases linearly with the overall sulfur content of the sample. This means that sulfur species other than covalently bonded sulfur are catalytically active sites for benzylation of toluene. These sulfur species have been identified as protonic sites in ionic configuration (Scheme 1). Therefore, we conclude that hydrated zirconia surface having ionic configuration are responsible for higher catalytic activity for the benzylation of toluene and not the covalent S=O sites. It is similar to the observations of Babou[30] who also reported the catalytic activity in the presence of water and in contrast to Moreterra[31] who stated that surface sulfate in ionic configuration do not induce catalytic activity in the sulfated zirconia system.

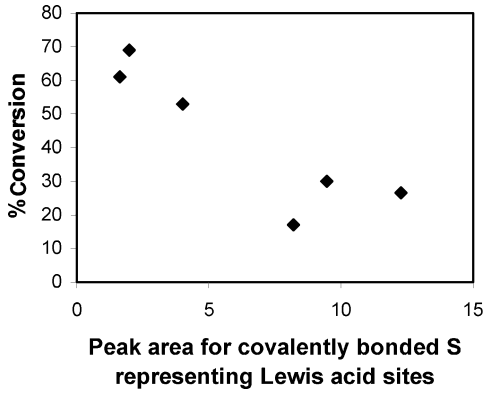

Figure 13. Correlation of covalently bonded sulfur representing Lewis acid sites with catalytic activity for benzylation of toluene.

Catalyst SZ-14, which had shown the highest benzylation activity, was regenerated by washing the used catalyst with acetone, followed by thermal activation at 723 K for 2 h. Conversion for benzylation of toluene with thus regenerated catalyst was found to be 35% with 100% selectivity for para isomer showing thereby that the catalyst is not regenerated by this method. The measured surface area for spent catalyst (SZ-14) after regeneration showed a decrease from 85 to 77 m^2/g.

Conclusions

The sol−gel technique has resulted in the formation of nanocrystalline sulfated zirconia catalyst having a low crystallite size (<20 nm) with tetragonal as a predominant phase. The amount of sulfur and the nature of the sulfur species bound with the zirconia surface play a significant role in determining the catalytic activity of a sample, which, in turn, depends on various synthetic parameters. Lower (<1%) sulfur loading results in higher covalently bonded sulfur character in sulfated zirconia catalysts. Sulfated zirconia samples with surface area (64−116 m^2/g) and pore size (47−67 Å) were obtained. Ultrasonication assisted sulfated zirconia samples prepared with higher concentration of the metal precursor were found to be superior in higher sulfur loading and dispersion and thus for higher catalytic activity for the benzylation of toluene. Ultrasonication also favors the formation of low crystallite size. In the present reaction conditions, benzylation of toluene was carried out by sulfur species having ionic configuration, which is attributed to high sulfur content and its highly sensitive nature towards molecular water.

Acknowledgment

Authors are thankful to NMITLI program of CSIR for supporting this work. We also express our thanks to Dr. P. K. Ghosh, Director CSMCRI, for his encouragement. Instrumental support for X-ray analysis from Dr. (Mrs.) P. A. Bhatt, sulfur analysis from Mr. R. J. Tayade, N_2 adsorption from Jince Sebastian, and C. D. Chudasama are acknowledged.

Literature Cited

(1) Tanabe, K. Solid Acid−Base Catalysts In *Catalysis Science and Technology*; Anderson, J. R., Boudart, M., Eds.; Springer-Verlag: New York, 1981; Vol. 2, Chapter 5.

(2) Hino, M.; Kobayashi, S.; Arata, K. Reactions of Butane and Isobutane catalysed by zirconium oxide treated with sulfate ion. Solid super catalyst. *J. Am. Chem. Soc.* **1979**, *101*, 6439.

(3) Hino, M.; Arata, K. Synthesis of solid acid catalysts with acid strength of $H_0 > -16.04$. *J. Chem. Soc. Chem. Commun.* **1980**, 851.

(4) Arata K. Solid superacids. *Adv. Catal.* **1990**, *37*, 165.

(5) Song, X.; Sayari, A. Sulfated zirconia-based strong solid-acid catalysts: Recent Progress. *Catal. Rev. Sci. Eng.* **1996**, *38*, 329.

(6) Yadav, G. D.; Nair, J. J. Sulfated zirconia and its modified versions as promising catalysts for industrial process. *Microporous Mesoporous Mater.* **1999**, *33*, 1.

(7) Parvulescu, V.; Coman, S.; Grange, P.; Parvulescu, V. I. Preparation and characterization of sulfated zirconia catalysts obtained via various procedures. *Appl. Catal. A* **1999**, *176*, 27.

(8) Wang, J. A.; Valenzyela, M. A.; Salmons, J.; Vazquez, A.; Garcia-Ruiz, A.; Bokhimi, X. Comparative study of nanocrystalline zirconia prepared by precipitation and sol−gel methods. *Catal. Today* **2001**, *68*, 21.

(9) Gomez, R.; Lopez, T. Dehydroxylation and the crystalline phases in sol−gel zirconia. *J. Sol-Gel Sci. Technol.* **1998**, *11*, 309.

(10) Gomez, R.; Lopez, T.; Ferrat, G.; Dominguez, J. M.; Schifter, I. pH effect on the preparation by sol−gel method of ZrO_2/SiO_2 catalysts. *Chem. Lett.* **1992**, 1941.

(11) Chadwick, A. V.; Mountjoy, G.; Nield, V. M.; Poplett, I. J. F.; Smith, M. E.; Strange, J. H.; Tucker, M. G. Solid-state NMR and X-ray studies of the structural evolution of nano-crystalline zirconia. *Chem. Mater.* **2001**, *13*, 1219.

(12) Ko, E. I. Sol−gel Process In *Preparation of Solid Catalysts in Handbook of Heterogeneous Catalysis*; Knozinger, G. Ertl, H., Weitkamp, J. Eds.; VCH Verlagsgesellschaft mbH, Weinhein, Vol. 2, Chapter 2, p 86.

(13) Brinker, C. J.; Scherer, G. W. *Sol−Gel Science*; Academic Press: San Diego, CA, 1990.

(14) Viswanathan, B.; Aulice Scibioh M. Nanomaterials: A new generation in material science. *Bull. Catal. Soc. India* **2001**, 11.

(15) Pathak, A.; Pramik, P. Nanoparticles of oxides through chemical methods. *PINSA-A: Proc. Indian Natl. Sci. Acad., Part A* **2001**, *67*, *1*, 47.

(16) Mishra, H. K.; Parida, K. M. Studies on sulphated zirconia: synthesis, physicochemical characterization and *n*-butane isomerisation activity. *Appl. Catal. A* **2002**, 224.

(17) Trung Tran, Gnep N. S.; Szabo, G.; Guisnet, M. Influence of the calcination temperature on the acidic and catalytic properties of sulphated zirconia. *Appl. Catal. A* **1998**, *171*, 207.

(18) Signoretta, M. M.; Oliva, L.; Pinna, F.; Strukul, G. Synthesis of sulfated zirconia aerogel: effect of the chemical modification of precursor on catalytic activity. *J. Non-Cryst. Solids* **2001**, *290*, 145.

(19) Melada, S.; Signoretta, M.; Ardizzone, S. A.; Bianchi, C. L. Physico-chemical features and catalytic activity of sulfated zirconia prepared by sol−gel method. The role of the solvent evaporation step. *Catal. Lett.* **2001**, *75*, 199.

(20) Cullity, B. D.; Stock, S. R. *Elements of X-ray Diffraction*, 3rd ed.; Prentice Hall: Upper Saddle River, NJ, 2001; p 388.

(21) Su, Caili.; Li, Junrong.; He, Dehua.; Cheng, Zhengxing.; Zhu, Qiming. Synthesis of isobutene from synthesis gas over nanosize zirconia catalyst. *Appl. Catal. A* **2000**, *202*, 81.

(22) Gregg, S. J.; Sing, K. S. W. *Adsorption, Surface Area and Porosity*, 2nd ed; Academic Press: New York, 1982.

(23) Duran, P.; Gonzalez, M.; Moure, C.; Jurado, J. R.; Pascual, C. Preparation, sintering and properties of translucent erbium oxide (Er_2O_3)- doped tetragonal zirconia. *J. Mater. Sci.* **1990**, *25*, 5001.

(24) Huang, Y-y.; Zhao, Bi-y.; Xie, Y-c. Preparation of zirconia-based acid catalysts from zirconia aerogel of tetragonal phase. *Appl. Catal. A.* **1998**, *172*, 327.

(25) Yamaguchi, T.; Jin, T.; Tanabe, K. Structure of acid-sites on sulfur- promoted iron oxide. *J. Phys. Chem.* **1986**, *90*, 3148.

(26) Ward, D. A.; Ko, E. I. One step synthesis and characterization of zirconia -sulfate aerogels as solid super acids. *J. Catal.* **1994**, *150*, 18.

(27) Bensitel, M.; Saur, O.; Lavalley, J. C.; Morrow, B. A. An infrared study of sulfated zirconia. *Mater. Chem. Phys.* **1988**, *19*, 147.

(28) Thompson, L. H.; Doraiswamy, L. K. Sonochemistry: Science and Engineering. *Ind. Eng. Chem. Res.* **1999**, *38*, 1215.

(29) Morterra, C.; Cerrato, G.; Bolis, V. Lewis and Bronsted acidity at the surface of sulfate-doped ZrO_2 catalysts. *Catal. Today* **1993**, *17*, 505.

(30) Babou, F.; Coudurier, G.; Vedrine, J. Acidic properties of sulfated zirconia: An infrared spectroscopic study. *J Catal.* **1995**, *152*, 341.

(31) Morterra, C.; Cerrato, G.; Pinna, F.; Signoretto, M.; Strukul, G. On the acid-catalyzed isomerisation of light paraffins over a ZrO_2/SO_4 system: The effect of hydration. *J. Catal.* **1994**, *149*, 181.

Received for review February 6, 2003
Revised manuscript received July 30, 2003
Accepted August 2, 2003

IE030099T